

Fossil steroids record the appearance of Demospongiae during the Cryogenian Period

Gordon D. Love, Emmanuelle Grosjean, Charlotte Stalvies, David A. Fike, John P. Grotzinger, Alexander S. Bradley, Amy E. Kelly, Maya Bhatia, William Meredith, Colin E. Snape, Samuel A. Bowring, Daniel J. Condon and Roger E. Summons

1. Overview

In this investigation, we monitored the stratigraphic occurrence and abundance of the fossil C_{30} steranes, 24-isopropylcholestanes^{S1}, in rock extracts and kerogen hydropyrolysates in the Huqf Supergroup in South Oman Salt Basin (SOSB) and used the absolute U-Pb zircon age framework^{S2} established for the host strata to better constrain the timing of the radiation of Porifera in the Neoproterozoic. GC-MS analysis of saturated hydrocarbon fractions with metastable MRM allowed investigation of the distributions of trace biomarker compounds, such as C_{26} and C_{30} steranes (Figure 2). The ratio of 24-isopropylcholestane / 24-*n*-propylcholestane (for all 4 regular geoisomers) was measured for extracts and pyrolysates and found to be anomalously high (0.52-16.1, with an average value of 1.51, Tables S1-S2) in all Neoproterozoic-early Cambrian SOSB samples in comparison with Phanerozoic and mid-Proterozoic oils and bitumens reported previously (typically $<0.3^{S1}$). Since the absolute abundances of steranes varies widely, the 24-*n*-propylcholestane marker for marine

pelagophyte algae^{S3} provides a molecular benchmark for inputs of sponge biomass to sediments through geological time. We propose that only a significant input from demosponges could result in such a consistently high value for this 24-iso / *n*-propylcholestane ratio found in our Huqf rock bitumens and kerogen hydropyrolysates. So, we are reporting the oldest continuous sponge biomarker record, representing ca. 100 million years of sedimentary deposition, with 24-iso/*n*-propylcholestane ratios all ≥ 0.5 for both rock bitumen and kerogen-bound biomarker pools.

Previous work^{S1} had established that a temporal pulse of elevated 24-iso/24-*n*-propylcholestane ratios (all > 0.5 and often around 1.0) existed in numerous sedimentary rocks from different basins of Neoproterozoic to Early Cambrian age (and later found in some Early Ordovician rocks), although the first occurrence of elevated amounts of this compound in the Neoproterozoic had not been well temporally constrained. Either side of this temporal pulse, ratios of 24-iso/24-*n*-propylcholestane > 0.5 have never been reported and the common background ratio is typically 0.2-0.3^{S1} (See Sections 10 and 11 for further discussion).

Low 24-iso / *n*-propylcholestane ratios (especially < 0.3 but also those < 0.5 come under scrutiny) should be treated with suspicion if this parameter is being used to advocate ancient sponge inputs, for reasons outlined in Section 10. Multiple analyses of rock samples from a particular stratigraphic interval or formation are also needed to verify that this is a consistent biomarker feature of the sedimentary rock unit. Ideally ratios of 24-iso / *n*-propylcholestane ≥ 0.5 should be consistently observed in multiple rock samples as a conservative rule of thumb

to unambiguously discern ancient demosponge inputs above the average background value (0.2-0.3) for ancient marine sedimentary rocks of all ages^{S1}

The parallel analysis of kerogen-bound products, containing abundant covalently bound 24-isopropylcholestanes (Table S2), alongside conventional solvent-extractable biomarkers adds significant confidence that these sponge biomarkers are indigenous and syngenetic with the host sediment and have not simply migrated from other, possibly younger, strata. The bound biomarker pool exhibits a slightly less mature distribution of hopanes and steranes than the corresponding solvent extracts for any particular rock, including noticeably less amounts of rearranged hopanes and sterane isomers (such as neohopanes and diasteranes)^{S4,S5}. This distinguishes the HyPy products from any residual rock bitumen components which may have escaped solvent extraction or any migrated petroleum and confirms that the HyPy-generated biomarkers were predominantly covalently-linked into kerogen. Furthermore, the kerogen-bound biomarker distributions confirm that kerogen was largely formed during early stages of diagenesis

While no obvious consistent stratigraphic or temporal patterns for sponge steranes were observed, the highest ratios of 24-iso / *n*-propylcholestane were found in the oldest strata analysed, the Masirah Bay and Ghadir Manquil Formations. These formations are found above and below the Marinoan cap carbonate, respectively (Figure 1- see page 11).

2. Justification for ancient demosponges being considered the only major biogenic source of 24-isopropylcholestanes in Neoproterozoic and Cambrian Huqf strata

The only reports in the lipid survey literature of 24-isopropylcholesterol from a biogenic source other than demosponges is for trace amounts (<0.4% of total sterols) in two species of unicellular marine pelagophyte algae (see Table S3)^{S6-S10}, but never in any other class of algae^{S11,12}. This restricted phylogenetic distribution is readily explained by reference to the biosynthetic pathway leading to C₃₀ sterols. Pelagophyceae are a small class of marine chromophyte algae which feature 24(E)-24-propylidenecholesterol as their dominant sterol^{S10}, the biosynthesis of which follows an unusual mechanism via a 3-carbon side chain cyclopropyl intermediate to achieve the required *n*-propyl side chain structure^{S6,13}. For pelagophyte algae, the 24-isopropylcholesterol is a minor by-product of the biosynthesis of the much more abundant sterol compounds containing a 24-*n*-propylcholestane skeleton (Table S3, predominantly 24-*n*-propylidenecholesterol but also get 24-*n*-propylcholesterol). It is an aberration of an enzymatic process intended to produce 24-*n*-propylidenecholesterol (and related structures) and does not constitute a biosynthetic capacity to make abundant 24-isopropylcholesterol given optimal growth conditions.

Table S3: Summary of quantitative sterol surveys performed on Pelagophyceae

Pelagophyte Species	total NPC	total IPC	Reference
<i>Pulvinaria</i> sp. [^]	47.32% [#]	0.31% [†]	Kokke et al. (1984) ^{S6}
<i>Aureoumbra lagunensis</i>	40.9%	0.4%	Giner et al. (2001) ^{S7}
<i>Pulvinaria</i> sp. [^]	29% (58%*)	Not detectable	Rohmer et al. (1980) ^{S8}
<i>Nematochrsopsis roscoffensis</i>	49%	Not detectable	Raederstorff & Rohmer (1984) ^{S9}
<i>Aureococcus anophagefferens</i>	44.4%	Not detectable	Giner & Boyer (1998) ^{S10}

IPC/NPC (from pelagophyte sterols or sterol esters) = 0.00 – 0.01

IPC/NPC (from Neoproterzoic-Cambrian steranes from Huqf) = 0.52- 16.1 (average = 1.51, n = 81 analyses)

NPC = steroids with 24-*n*-propylcholestane skeleton

IPC = steroids with 24-isopropylcholestane skeleton

[^] *unclassified chrysophyte* in original studies but later reclassified as *Pulvinaria* sp. (Saunders et al., 1997)

* 58% of total sterol esters were NPC. (29% of free sterols were NPC)

[#] combined sterol and sterol ester analyses

[†] trace sterols, including IPC, became detectable when a higher mass of cell biomass was extracted

Variations in sterol composition of microalgae are generally small^{S12} and there is no evidence that the relative abundance of 24-isopropylcholesterol might vary by the two orders of magnitude range needed to invalidate the general finding of 24-*n*-propylidenecholesterol dominance in pelagophytes. In contrast to pelagophytes, numerous genera of extant marine demosponges still produce 24-isopropylcholesterols (and related structures) as their major sterols (including *Pseudaxynissa* sp. for which they routinely comprise 99% of total sterol content, see Section 9). Since the 24-iso / *n*-propylcholesterol ratio (the precursor sterol version of the fossil sterane ratio that we used in SOSB) is only 0.01 or less for screened pelagophytes, then clearly the much higher fossil ratios (average of 1.51 for extracts plus kerogen pyrolystaes) found in all formations of the Huqf Supergroup in SOSB are highly unlikely to be attributable to marine algal inputs.

Consistent with this viewpoint, although marine pelagophytes are common primary producers in oceans throughout the Phanerozoic to present, elevated ratios of 24-iso / *n*-propylcholestanes (>0.5, and frequently >1.0) have only been recorded in Neoproterozoic to Ordovician age sediments (with the main pulse recorded from Ediacaran-Early Cambrian). Thus, these elevated 24-iso / *n*-propylcholestanes are most likely recording a specific biogenic input (demosponges). Sediments and oils younger than Ordovician or older than Sturtian age (ca. 713 Myr) do not contain elevated amounts of 24-isopropylcholestanes even though they do contain 24-*n*-propylcholestanes (signifying pelagophyte contributions). This strongly suggests that marine pelagophytes or any other algae are incapable of making abundant 24-isopropylcholesterol relative to sterols with the 24-*n*-propylcholestane skeleton, regardless of

environmental growth conditions. So, ancient demosponge inputs are by far the most parsimonious explanation of the anomalously high 24-iso / 24- *n*-propylcholestanes reported in our data set (Tables S1 and S2- see pages 48-50).

3. Huqf Supergroup, South Oman Salt Basin

The Huqf Supergroup provides one of the best preserved, most continuous sections of late Neoproterozoic through earliest Cambrian strata (ca. 710 – 540 Myr)^{S14-S16}. Huqf strata are preserved both in surface outcrops of the Oman Mountains and the Huqf area, and within subsurface sedimentary basins, most prominently the South Oman Salt Basin (SOSB)^{S17}. The South Oman Salt Basin located at the southeastern edge of the Arabian peninsula is developed on ca. 840 to ca. 810 Myr Pan-African basement^{S2}. The Huqf Supergroup^{S15} begins with a thick glaciogenic siliclastic unit (Abu Mahara Group), followed by two clastic-carbonate cycles (Nafun Group) and is capped by a chert-carbonate evaporite succession (Ara Group) (Figure 1-see page 11).

The Abu Mahara Group contains the Sturtian-equivalent (Ghubrah Formation) and the Marinoan-equivalent (Fiq Formation) glacial deposits. In the subsurface, the Abu Mahara consists of the Ghadir Manquil Formation, which encompasses both glacial episodes. The Abu Mahara strata were deposited in localized rift basins^{S18}. In Oman, these two glacial periods have been dated to ca. 713 and < 645 Myr, respectively^{S2,S19}. There is no preserved Sturtian cap carbonate above the Ghubrah glacial deposits; rather, the Ghubrah is truncated by a volcanic unit (Saqlah Formation) that separates the two glacial periods^{S20,S21}. The Fiq

Formation, however, has a well developed cap carbonate (Hadash Formation)^{S22,S23}, which is traceable throughout the subsurface.

The overlying Nafun Group sediments were deposited in a regionally extensive sag basin under open, shallow marine conditions, and each formation can be traced laterally for several hundred km across Oman^{S16,S24-S26}. Nafun Group strata comprise two clastic-to-carbonate shallowing-upward successions (Masirah Bay Formation and Khufai Formation; Shuram Formation and Buah Formation) with an unconformity across the Khufai-Shuram boundary^{S16}. The basal Shuram has a firm maximum age of ca. 620 Myr based on the age of two detrital zircons^{S2,S27} and the Khufai-Shuram contact is believed^{S2} to include the interval of Gaskiers glaciation at ca. 580 Myr^{S28}, although Le Guerroue et al.^{S25,S27} argue for continuous deposition across this contact. The upper Nafun Group contains the Shuram excursion, a >15‰ negative excursion in $\delta^{13}\text{C}_{\text{carb}}$ that spans ~ 500m from the basal Shuram Formation through the mid-Buah Formation^{S25,S29,S30}. This distinctive isotopic signature makes the Shuram excursion a useful marker for both regional and global chemostratigraphic correlation^{S30-S36}. Global correlation of $\delta^{13}\text{C}_{\text{carb}}$ anomalies provides two age constraints for the Buah Formation: ca. 550 Myr for the mid-Buah (correlation with Doushantuo Formation, China^{S2,S32}); and ca. 548 Myr for the upper Buah (correlation with Nama Group, Namibia^{S2,S37}). These ages are consistent with those obtained from the overlying Ara Group.

The Ara Group consists of a series carbonate-evaporite sequences deposited in strongly subsiding block-faulted basin^{S24,S38}. A detailed description of the paleogeography and

stratigraphy of the Ara group is available in Schroeder & Grotzinger^{S39}. Briefly, during deposition of the Ara group, the SOSB was subdivided into three separate palaeogeological domains: two carbonate platforms referred to as the North and South Platforms, separated by a deep basin (Athel basin) with water depths potentially of several hundred meters in the deeper depocentres^{S26}. The carbonate platforms consist of a cyclic succession of up to six carbonate units, or ‘stringers’, each sandwiched by evaporites^{S26}. The carbonate-evaporite cycles are termed A1 to A6 from oldest to youngest and were deposited between ca. 547 – 540 Myr^{S2}. Ara Group and E-C boundary strata are known definitively only from the subsurface^{S26,S40}. The presence of multiple ash horizons within Ara Group strata has significantly improved our understanding of the timing and duration of Ara deposition and our ability to correlate the Oman stratigraphy with other sections globally^{S2,S37,S40}. An age of 546.72 ± 0.22 Myr comes from the middle of the basal (A0) Ara carbonate^{S2}. Ash beds at the base^{S2,S40} and top^{S2} of the third carbonate unit (A3) yield zircon U/Pb ages of 542.91 ± 0.13 and 542.31 ± 0.14 Myr, respectively. The base of the A4 carbonate unit contains an ash that yielded a U/Pb age^{S2,S40} of 541.00 ± 0.12 Myr. This age, in combination with a 7‰ negative excursion in carbonate $\delta^{13}\text{C}$ and the disappearance of Ediacaran *Namacalathus* and *Cloudina* fossil assemblages, is the basis for the identification of the E-C boundary at the base of the A4 carbonate in Oman^{S40}.

In the basin centre (Athel basin), the stratigraphic equivalent of the A4 unit consists of two organic-rich shale units, the U shale and the Thuleilat shale that bracket the unique siliceous rocks of the Athel silicilyte (a.k.a. Al Shomou silicilyte)^{S39,S40}. On the basin margin (termed the Eastern Flank) of the SOSB, Ara Group strata are recorded as a series

of evaporite-free carbonates. There is a robust correlation^{S14} between the Ara carbonates interbedded with evaporites on the interior of the SOSB and those deposited on the Eastern Flank, based on the presence of an ash-bed dated to 541 Myr^{S2}, $\delta^{13}\text{C}_{\text{carb}}$ chemostratigraphy, drill core logs, and trace element geochemistry. In both the SOSB and the Eastern Flank, the contact between the Buah and overlying Ara Group is marked by a disconformable, karstic surface that represents less than ~ 1 Myr^{S2}.

4. Sedimentary rocks used in this study

Petroleum exploration and production activities of Petroleum Development of Oman allowed us to access numerous deep (1-5 km) sediment cores and cuttings through the Huqf Supergroup as well as oils produced from these thermally well-preserved sediments. The sediments deposited within the Ara Group are commonly called *intra-salt* rocks, whereas rocks deposited before, including those of the Nafun Group, are referred to as *pre-salt* rocks. Ara source rocks deposited in the Athel Basin are commonly referred to as *Athel intra-salt* rocks, as opposed to the Ara carbonate stringers.

64 SOSB source rocks were provided in total (Tables S1 and S2), selected to provide extensive stratigraphic coverage (Figure 1) of all formations of the Huqf Supergroup in SOSB. Most of the samples were cuttings composites in order to more completely characterize the geochemistry of source rock intervals but some core material was also used. Rocks analysed had total organic contents (TOCs) of 0.2 to 11 wt% and the sedimentary organic matter was thermally well preserved, with Hydrogen Indices (HIs) measured from Rock-Eval pyrolysis in the range of 250-700 mg/g TOC^{S41}. These HI

values are typical of marginal- to middle-oil window source rock maturity and SOSB rocks represent the least thermally altered Neoproterozoic-Cambrian age sediments used to date for molecular biomarker work^{S41}.

5. Age constraints for the oldest sedimentary rocks containing demosponge steranes

A new maximum age for the top of the Marinoan diamictite in SOSB, just below the Marinoan cap carbonate from the Lahan-1 core, of <645 Myr has recently been reported from U-Pb detrital zircon geochronology^{S2}. This is compatible with an apparently synchronous age for the Marinoan cap carbonate worldwide from dated ash beds layers in Namibia and South China at *ca.* 635 Myr^{S32}. It remains unclear whether Sturtian-type glaciations represent a single, globally synchronous glacial epoch but the Huqf Supergroup contains evidence for two distinct Neoproterozoic glaciations, with the *ca.* 713 Myr age from the Gubrah Formation in Oman^{S2} being the first direct high precision age constraint for a 'Sturtian' age Neoproterozoic glacial deposit. A thin dolostone layer, characterized by depleted $\delta^{13}\text{C}$ carbonate atop diamictite and below the shales of the Masirah Bay Fm. and interpreted as Marinoan cap carbonate, was found in both GM-1 and MQR-1 wells from which the sedimentary rock samples used as representatives for Ghadir Manquil Fm were taken (Figure S1 - see next page).

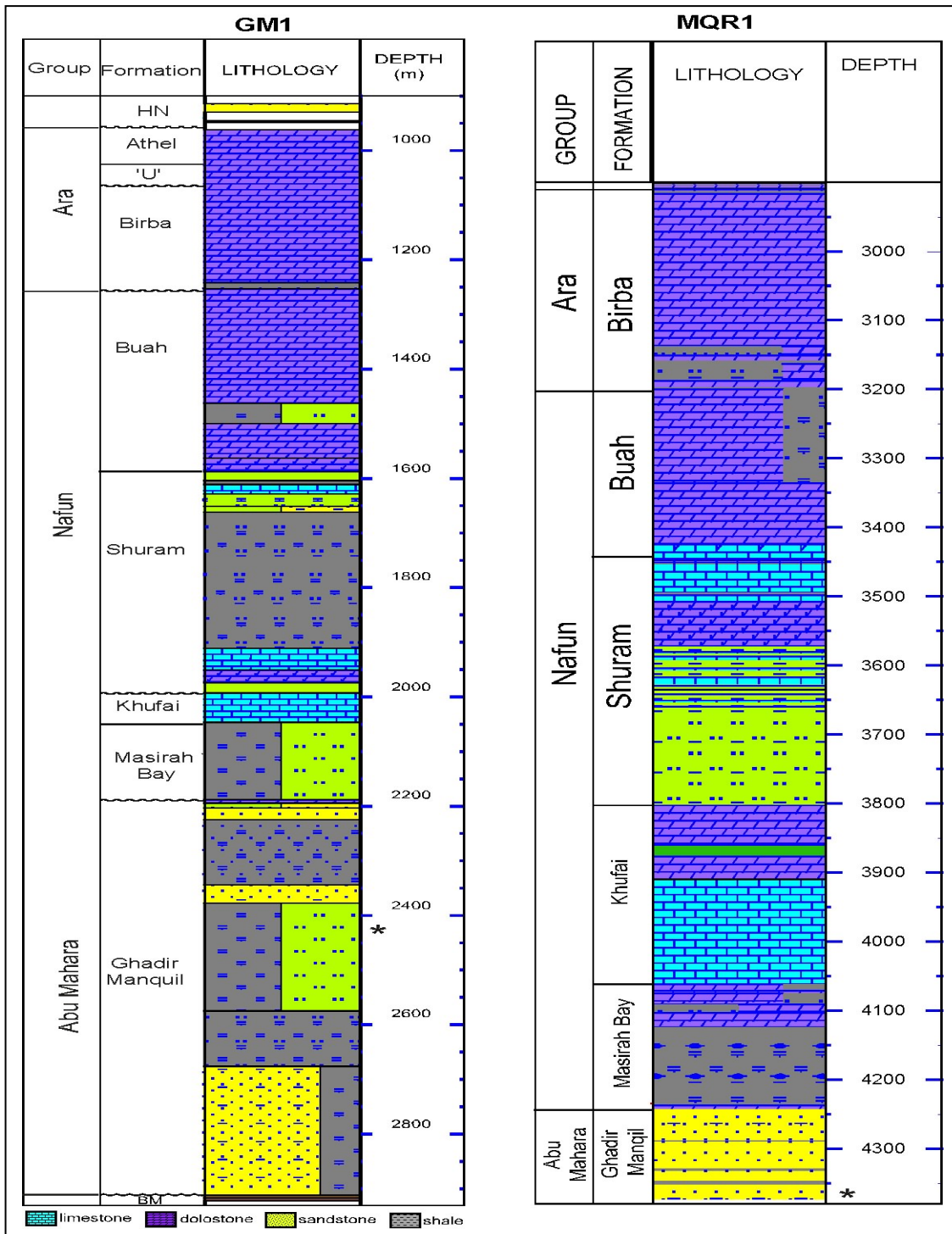


Figure S1. (See over for legend)

Figure S1. Stratigraphic column for wells containing late Cryogenian (pre-Ediacaran) evidence for sponges in sediments from a) well GM-1. b) well MQR-1. * denotes stratigraphic position of sedimentary rocks used for biomarker work.

The Ghadir Manquil Fm. sediment from GM-1 core was a lime mudstone found approximately 150 metres below the base of a diamictite that we interpret as Marinoan age because of the stratigraphic position directly beneath both the Nafun Gp sedimentary package and the underlying (Marinoan) cap carbonate. The MQR-1 sedimentary rock was a siltstone/sandstone also found below the same sedimentary units in this well. So, we interpret the age of both these Ghadir Manquil Fm. sediments, and hence the age of our oldest demosponge biomarkers, as being younger than the Sturtian diamictite (*ca.* 713 Myr) but older than the Marinoan cap carbonate (*ca.* 635 Myr). A detrital age of 751 Myr from a single zircon grain from the GM-1 sample constrains an absolute maximum age for the Cryogenian sponge markers found in our study.

The GM-1 sample was interpreted to contain predominantly primary biomarker signal, from the high C₂₉ sterane (stigmastane) content and high 24-isopropyl/n-propylcholestanes ratio (Tables S1 and S2) and the good match of biomarker features with kerogen products. The MQR-1 well cuttings sample contained a mixture of primary signal and organics from a petroleum-derived lube oil used in drilling which we recognized from the appearance of anomalous biomarker features (such as higher levels of rearranged steranes and hopanes than normal plus baseline rise in GC profiles due to enhanced unresolved complex mixture components).

Note, from the lowest value of 24-iso / *n*-propylcholestane for MQR-1 extract of 0.52 (Table S1), that the net result of any substantial organic contamination with petroleum-derived additives is to reduce the abundance of 24-isopropylcholestanes relative to 24-*n*-propylcholestanes. This is not surprising since 24-isopropylcholestanes are generally absent or present in only trace quantities in marine Phanerozoic-sourced oils younger than Ordovician^{S1}, from which the lubricating fluids are typically derived. Thus, the high ratios of 24-iso / *n*-propylcholestane detected in SOSB over a 100 Myr period from the late Cryogenian to early Cambrian are genuine biomarker signals which record significant demosponge inputs at the time of deposition of the host sediment and cannot arise from contamination effects.

For the GM-1 sample, significant quantities of 24-isopropylcholestanes were also detected in the kerogen hydropyrolyste (Table S2) as for all other samples analysed. Kerogen-bound biomarkers are much less susceptible to contamination issues than extractable hydrocarbons since (i) kerogen is formed rapidly in geologic time, with formation commencing in the water column and the macromolecular organic matter being largely in place over a timescale of hundreds to thousands of years of sub-surface burial after deposition^{S42}, and (ii) the most common organic contaminants pervading into ancient sediments are soluble and mobile molecular species (e.g. *in-situ* migrated petroleum or refined petroleum-derived additives introduced during sample collection and storage and product work-up). Our kerogen biomarker data provide further confirmation that the characteristic biomarker features found in solvent extracts from Huqf sediments from the

SOSB, such as stigmastane dominance arising from green microalgal inputs and abundant 24-isopropylcholestanes from demosponges, are genuine biomarker signals indicative of source biota.

EXPERIMENTAL

6. Sediment preparation and extraction

The outer surfaces of sediment core and larger cuttings fragments were cleaned sequentially by ultrasonication in distilled water, then methanol, then dichloromethane, and finally *n*-hexane for ~20 seconds per step prior to extraction. Cleaned core fragments and cuttings were then crushed to a fine powder using an alumina ceramic puck mill housed in a SPEX 8510 shatterbox. Between samples, the puck mill was cleaned by crushing annealed sand three times for 1-minute periods each followed by washing with the same cleaning solvent sequence described above.

Rock powders were extracted with a mixture of dichloromethane and methanol (9:1, v/v) using a Dionex Accelerator Solvent Extractor ASE-200 operated under 1000 psi at 100 °C. Asphaltenes were precipitated out from the resulting organic extracts (bitumens) and from the oils using *n*-pentane. In asphaltene-free fractions (maltenes) derived from bitumens, elemental sulphur was removed with activated and solvent-washed copper pellets. The maltenes were then fractionated on silica gel column by liquid chromatography eluting successively with hexane, hexane/CH₂Cl₂ (v/v: 8:2) and CH₂Cl₂/CH₃OH (v/v: 7:3) to yield respectively saturated hydrocarbons, aromatic hydrocarbons and resins.

7. Catalytic hydropyrolysis of kerogen in sediments

Continuous-flow hydropyrolysis experiments were performed on 100–2000 mg of catalyst-loaded pre-extracted sediments or kerogen concentrates as described previously^{S4}. The isolation of kerogen concentrates was conducted on solvent-extracted rock residues by standard hydrofluoric acid/ hydrochloric acid (HF/HCl) extraction procedures. Further treatment of the isolated kerogens involved extraction with dichloromethane by ultrasonication ($\times 3$). Extracted sediments and kerogens were initially impregnated with an aqueous methanol solution of ammonium dioxodithiomolybdate $[(\text{NH}_4)_2\text{MoO}_2\text{S}_2]$ to give a nominal loading of 2 wt% molybdenum. Ammonium dioxodithiomolybdate reductively decomposes *in situ* under HyPy conditions above 250°C to form a catalytically-active molybdenum sulphide (MoS_2) phase.

The catalyst-loaded samples were heated in a stainless steel (316 grade) reactor tube from ambient temperature to 260°C at 300°C min^{-1} then to 500°C at 8°C min^{-1} . A hydrogen sweep gas flow of 6 $\text{dm}^3 \text{min}^{-1}$, measured at ambient temperature and pressure, through the reactor bed ensured that the residence times of volatiles generated was the order of only a few seconds. Products were collected in a silica gel trap cooled with dry ice and recovered in dichloromethane (DCM) for subsequent fractionation using silica gel adsorption chromatography.

To reduce the levels of background contamination in HyPy, a cleaning run was performed before each sample run whereby the apparatus was heated to 520°C using a rapid

heating rate ($300^{\circ}\text{C min}^{-1}$) under high hydrogen pressure conditions. Experimental blanks, using annealed silica gel in the reactor tube instead of a kerogen sample, were regularly performed and the products monitored and quantified to ensure that trace organic contamination levels were acceptably low.

8. Biomarker analyses

8.1 Ancient sedimentary rocks from SOSB

Product fractionation: Maltenes prepared from rock extracts were first treated by addition of solvent-washed activated copper turnings to remove traces of elemental sulfur and then separated by silica gel adsorption chromatography into saturates, aromatics and polars (or N, S, O compounds) by elution with *n*-hexane, *n*-hexane-dichloromethane (4:1 v/v) and dichloromethane-methanol (3:1 v/v), respectively. For hydropyrolsates, solvent-extracted, activated copper turnings were added to concentrated solutions of saturate hydrocarbon fractions to remove all traces of elemental sulfur, which is formed from disproportionation of the catalyst during HyPy.

For a sub-set of the rock extracts where *n*-alkanes dominated the biomarker signal, branched and cyclic saturated hydrocarbons were separated from straight-chain alkanes by treating the saturated hydrocarbon fraction with silicalite molecular sieve. Approximately 5-10 mg of saturated hydrocarbons, dissolved in a minimum volume of *n*-pentane was placed on a 3 cm bed of activated, crushed silicalite lightly packed into a Pasteur pipette. The silicalite non-adduct (SNA) containing branched and cyclic alkanes was washed through using pentane (4 ml).

A deuterated C₂₉ sterane standard (d₄-- $\alpha\alpha\alpha$ -24-ethylcholestane (20R), Chiron Laboratories AS) was added to branched/cyclic alkane or total saturate fractions prior to gas chromatography-mass spectrometry (GC-MS) to quantify biomarker peaks, with typically 50 ng internal standard added to a 1 mg aliquot of saturates. Strictly, saturated fractions produced from HyPy should be termed *aliphatics* (as they contain both saturates and lower amounts of alkene products) but for simplicity we will use the term *saturates* to describe the first product fraction (as alkanes are dominant over alkenes) that elutes with hexane, even for hydropyrolysates.

Gas Chromatography-Mass Spectrometry: GC-MS analyses on aliphatic hydrocarbon fractions were carried out on a Micromass AutoSpec Ultima equipped with a HP6890 gas chromatograph (Hewlett Packard) and a DB-1MS coated capillary column (60 m x 0.25 mm i.d., 0.25 μ m film thickness) using He as carrier gas. The MS source was operated at 250°C in EI-mode at 70 eV ionization energy and with 8000 V acceleration voltage. Samples were injected in pulsed splitless mode into a Gerstel PTV injector at a constant temperature of 300°C. For full-scan and selected ion recording (SIR) experiments, the GC oven was programmed at 60°C (2 min), heated to 315°C at 4°C/min, with a final hold time of 35 min. The AutoSpec full-scan duration was 0.8 s plus 0.2 s interscan delay over a mass range of 50 to 600 Da. Hopane and sterane biomarkers were analyzed by metastable reaction monitoring (MRM) with a total cycle time of 1.3 s per scan for 26 precursor-product transitions, including m/z 414 to 217 transition for C₃₀

desmethylsteranes. For MRM, the GC oven was programmed at 60°C (2 min), heated to 150°C at 10°C/min, further heated to 315°C at 3°C/min and held at the final temperature for 24 min.

Peak identifications of sponge steranes were confirmed by comparison of retention times with an AGSO oil saturated hydrocarbon standard and with Neoproterozoic oils from Siberia^{S1} shown previously to contain significant quantities of 24-isopropylcholestanes. Polycyclic biomarkers were quantified assuming equal mass spectral response factors between analytes and the d₄-C₂₉- $\alpha\alpha\alpha$ -ethylcholestane (20R) internal standard. Analytical errors for absolute yields of individual hopanes and steranes are estimated at $\pm 30\%$. Average uncertainties in hopane and sterane biomarker ratios are $\pm 8\%$ as calculated from multiple analyses of a saturated hydrocarbon fraction prepared from an AGSO standard oil (n = 30 MRM analyses).

8.2 Analysis of sterols in modern sponge cells

Nine modern sponge samples (*Halichondria sp.*, *Suberites sp.*, *Cliona sp.*, *Microciona sp.*, *Dysidea fragilis*, *Clypeatula cooperensis*, *Leucosolenia sp.*, *Scypha lingua*, *Axinella sp.*) were acquired for extraction to monitor their free sterol contents. All sponges were supplied by Kevin Peterson (Dartmouth) and Erik Sperling (Yale), except for *Dysidea fragilis* from Ted Molinski (UCSD), and biomass arrived immersed in ethanol. Combined ethanol washings for each sample were filtered to remove suspended particulates,

concentrated by rotary evaporation into a small volume (a few mls) and then transferred to a pre-weighed 4 ml glass vial and blown down carefully under dry N₂ gas.

The ethanol-extracted sponge tissue was then freeze-dried and pulverized to a powder and further extracted using a modification of the Bligh-Dyer method^{S43}. The biomass powder (0.1-60 g) was then weighed and transferred to pre-solvent washed 50 ml Teflon tubes. Subsequently, 19 ml of a 10:5:4 mixture of methanol:chloroform:water was added to each sample in the Teflon tubes. Each tube was vortexed for 5 minutes and sonicated for 20 minutes before centrifugation at 5000 rpm for 5 minutes. The liquid phase was transferred to a 60-ml precombusted glass tube and the process was repeated at least twice with the remaining biomass. On the third extraction, 19 ml of a 10:5:4 mixture of methanol:chloroform:dichloromethane-washed water with 1% trichloroacetic acid (TCA) was used. The process was repeated until the extract color was clear.

Bligh-Dyer and ethanol extracts were typically combined to form a total lipid extract (TLE) before being separated into 5 fractions, based on polarity, by silica gel chromatography. Approximately, 3.0-4.0 mg of each TLE was adsorbed on the top of a 10 cm silica gel pipette column and then sequentially eluted with 1.5 column volumes of *n*-hexane, 2 column volumes of 8:2 *n*-hexane:dichloromethane, 2 column volumes of dichloromethane, 2 column volumes of dichloromethane:ethyl acetate, and finally 3 column volumes of 7:3 dichloromethane:methanol. The alcohol products, including sterols, typically all eluted in fraction 4 and approximately 20 µg of this fraction was derivatized

with 10 μl of bis(trimethylsilyl)trifluoroacetamide (BSTFA) in 10 μl of pyridine at 70°C for 30 minutes. Prior to derivatization, 100 ng of epiandrosterone was added as an internal standard.

Alcohol fractions were then analysed by GC-MS as trimethylsilyl (TMS) ethers within 36 hours of derivatization. 1 μl of the derivatized alcohol fraction (dissolved in 20 μl volume ethyl acetate) was analyzed via programmed-temperature vaporization (PTV) injection on to a 60 m Varian Chrompak CP-Sil 5CB capillary column (i.d. = 0.32 mm; film thickness = 0.25 μm) with He used as the carrier gas. The oven temperature program used for GC for the polar fractions (fractions 3-5) consisted of an initial temperature hold at 60°C for 2 min, followed by an increase to 100°C at 10°C·min⁻¹, and then a subsequent increase to 320°C at 4°C·min⁻¹ for 30 min. Data was analyzed using Chemstation G10701CA (Version C) software, Agilent Technologies.

1-2 g of ethanol-extracted sponge biomass for each sample was filtered and impregnated with an aqueous methanol solution of ammonium dioxodithiomolybdate [(NH₄)₂MoO₂S₂] to give a nominal loading of 2 wt% molybdenum prior to HyPy treatment. HyPy is also an excellent screening tool for assessing the variety of lipid types present in cell biomass by generating hydrocarbon skeletons from functionalized lipids^{S44}. A significant proportion of unsaturation in sterols are hydrogenated under HyPy conditions releasing sterane products (as well as steranes and diasterenes)^{S44}. Aliphatic fractions (alkanes plus alkenes) were isolated from total products using silica gel chromatography by

eluting with *n*-hexane and biomarker hydrocarbon products were analysed by full scan and MRM-GC-MS on the Autopsec as described for the Oman rock extracts and hydropyrolysates.

RESULTS & DISCUSSION

9. Significance of elevated 27-norcholestanes in SOSB sedimentary rocks

As well as containing the 24-isopropylcholestane markers for demosponges, all our SOSB sedimentary rock samples contained anomalously high amounts of another side chain-modified fossil steroid, 27-norcholestane, in both solvent extracts and kerogen hydropyrolysates (Tables S1 and S2). Precursor sterols of this fossil hydrocarbon, including 27-norcholesterol and polyunsaturated counterparts, have been reported previously from the marine demosponge, *Axinella cannabina*^{S45}. So, we investigated the possibility that elevated amounts of 27-norcholestanes in SOSB rocks (total C₂₆ steranes, typically dominated by 27-norcholestane, constituted on average 6.7% of total C₂₆-C₂₉ steranes, Table S1, in contrast to levels of <3% in most other oil- window-mature sediments and petroleum of any age), may also represent another molecular indicator of fossil demosponge input. For this reason, we monitored the free sterol distributions for a selection of modern sponges and screened the biomass for lipid content using HyPy (Table S3).

C₂₆ and C₃₀ sterols were typically found to constitute <2% of total C₂₆-C₃₀ sterols in the nine sponges analysed as measured from peak areas from total ion chromatograms (TICs). Cholesterol was often the most abundant sterol in sponge extracts, although C₂₈ and C₂₉

phytosterols (presumably obtained largely from dietary uptake) were also prominent and were found to be more abundant than cholesterol in some samples. The most common forms of C₂₆ monohydroxy sterols detected in our demosponge extracts had unsaturations at Δ 22 and Δ 5,22. C₂₆ sterols follow the higher carbon number homologs (particularly C₂₇) as regards unsaturation patterns; with Δ 5,22 being the most abundant C₂₆ sterol form when Δ 5-C₂₇ sterols dominate but with Δ 22-C₂₆ sterols preferred when C₂₇ stanols are more abundant, a pattern consistent with previous sterol surveys of the Demospongiae^{S46}.

The finding of C₂₆ sterols in sponge extracts does not necessarily imply the presence of 27-norcholestane skeleton since 24-norcholesterols are also commonly found as molecular constituents of sponge biomass, presumably reflecting an algal source from dietary uptake^{S47}. The diatom *Thalassiosira aff. antartica* and the dinoflagellate *Gymnodinium simplex* are both biological sources of 24-norcholesta-5,22-dien-3 β -ol^{S47}, so planktonic sources of C₂₆ sterols are also possible. HyPy generation of steranes was needed to discriminate the different C₂₆ sterol (21-, 24- and 27-norcholesterols) and C₃₀ sterol (24-isopropylcholesterols and 24-*n*-propylcholesterols) structural isomers since the derivatised sterols (as trimethylsilyl ethers) co-elute on standard capillary GC columns while the sterane forms can be resolved and detected by MRM-GC-MS.

HyPy experiments on a small set of modern sponges (Table S4) suggest that sterols containing a 27-norcholestane hydrocarbon skeleton may actually be more commonly distributed lipids in modern demosponges than 24-isopropylcholesterols. Cholesterol and

cholestanol model compounds were both pyrolysed under standard HyPy conditions to monitor the level of side chain cleavage produced by thermal cleavage during pyrolysis (by measuring the ratio of 27-norcholestane/cholestane products using MRM-GC-MS). The amount of side chain scission which occurred was found to be negligible in comparison to the amounts of 27-norcholestanes produced by the sponges.

Table S4. Screening of sponges using HyPy to assess their capacity to biosynthesise 27-norcholestane and 24-isopropylcholestane skeletons as sterols.

Genus	Class	Environment	C ₂₆ sterols [#]	C ₃₀ sterols [#]	27-norcholestane*	24-isopropylcholestane*
Halichondria	Demosponge	Marine	✓	✓	✓	x
Suberites	Demosponge	Marine	✓	✓	✓	x
Cliona	Demosponge	Marine	✓	✓	✓	x
Microciona	Demosponge	Marine	✓	✓	✓	x
Dysidea	Demosponge	Marine	✓	✓	✓	✓
Axinella	Demosponge	Marine	✓	✓	✓	✓
Clypeatula	Demosponge	Freshwater	trace	x	✓	x
Leucosolenia	Calcisponge	Marine	x	x	n.d.	n.d.
Scypha	Calcisponge	Marine	?	x	n.d.	n.d.

from analysis of TMS-derivatives of alcohols isolated from combined EtOH and Bligh-Dyer extracts

* detected in HyPy hydrocarbon products

n.d.: this sponge was not subjected to HyPy treatment

?: Scypha sp. contained trace amounts of C₂₆ sterols but which were likely the result of contamination from demosponges (Peterson, personal communication).

✓ indicates a positive identification

X indicates no discernible traces of these in HyPy products).

So, while we confirmed that 27-norcholesterols were present in significant quantities above detection limits and HyPy experimental controls for all 7 demosponges screened, the overall abundance of these compounds was low (<1%) relative to the major sterols such as cholesterol and cholestanol. Indeed, the low ratio of 27-norcholestanes to C₂₆-C₂₉ steranes

in sponge HyPy products (<1%) suggests that sponge input alone cannot account for the high levels of these fossil compounds in SOSB sediments (on average 6.7% of total extractable C₂₆-C₂₉ steranes) unless 27-norcholesterols were much more abundant sterol components in the Neoproterozoic sponges compared with modern sponges.

For C₃₀ monohydroxy sterols, two resolvable peaks with Δ 24(28) and, particularly, Δ 5, Δ 24(28) unsaturations were detectable and these compounds were mainly equivalent to 24-*n*-propylidenecholesterol and related sterols shown previously to be biosynthesized by marine pelagophyte algae^{S3}, although lower amounts of co-eluting sterols containing a 24-isopropylcholestane skeleton were inferred from HyPy studies. Furthermore, only *Dysidea fragilis* and *Axinella* sp. yielded detectable amounts of 24-isopropylcholestanes (with the immature $\alpha\alpha\alpha$ R and $\beta\beta\alpha$ R diastereoisomers dominant) from HyPy of sponge cells. The release of 24-isopropylcholestanes from HyPy of cells of *Dysidea fragilis* here is consistent with a previous report of abundant sterols containing the 24-isopropylcholestane carbon skeleton in another related species, *Dysidea herbacea*^{S48}. Thus, it appears that C₃₀ sterols synthesized *de novo* by sponges containing the 24-isopropylcholestane skeleton may actually be rarely found in modern sponges but when they do occur they are produced only by certain demosponge genera^{S1}.

Several modern sponge genera including *Dysidea* sp. (from the G1demosponge clade^{S80}), *Verongia* sp. (a G2 taxon^{S80}), *Druinella* sp., (a junior synonym of *Pseudoceratina* sp., G2^{S80}), *Pseudaxinyssa* sp. (a junior synonym for *Axynissa* sp., G4^{S80}), and *Trachyopsis*

sp. (a junior synonym for *Halichondria sp.*, $G4^{S80}$), still produce 24-isopropylcholesterol (and related sterols) amongst their most abundant cell membrane sterols^{S1,S49}. Thus, demosponge species containing abundant 24-isopropylcholesterol (and related structures) are distributed across three of the main demosponge clades (*G1*, *G2* and $G4^{S80}$). These include spiculated and unspiculated (*G1*) taxa. The earliest sponges may have been sub-millimetre to a few millimetre body size and possibly unspiculated^{S51}. The absence of 24-isopropylcholesterols in the one choanoflagellate species tested^{S68}, together with the distribution patterns for demosponge noted above, suggests that abundant 24-isopropylcholesterols in cell membranes are confined to demosponges and may have been a characteristic of the earliest demosponges. A report of significant amounts of 24-isopropyl-5 α (H)-cholest-22-en-3 β -ol (although this compound structure was only “tentatively identified”) in a Recent freshwater lake sediment^{S81} was most likely sourced by freshwater demosponges, of which there are many genera and species. Sterols containing a 24-isopropylcholesterane skeleton have been reported previously from freshwater sponges^{S82}.

In the case of *Pseudaxynissa sp.*, 24-isopropylcholesterol and 22-dehydro-24-isopropylcholesterol together may comprise more than 99% of total sterols^{S49} (suggesting a structural role for these sterols in the cell membrane). In contrast, 27-norcholesterols are always apparently minor sterol constituents (<1%) of total sterols in sponges^{S45}.

The earliest demosponges to appear may have possessed extremely small body sizes with sub-millimetre to a few millimetre dimensions^{S50} and so may not have required

siliceous spicules for protection and structural support, but instead possessed a proteinaceous skeleton made of spongin^{S51}. A diverse array of unconventional steroids found in demosponges^{S1,S45,S48,S49}, may reflect necessary membrane structural modifications that accompanied the important evolutionary transition from single celled protists to multicellular animals. The precise role that these unusual sterols, with structural modifications to the side chain or steroid nucleus, serve in demosponge cell membranes is not known but it has been suggested^{S52} that they may (i) fulfill a purely structural role by providing improved conformational alignment of cell membrane molecules, including other unusual sponge lipids and proteins, or alternatively, (ii) be involved in modulating a variety of physiological regulatory processes. In contrast to demosponges, a previous investigation into the sterol constituents of 20 Hexactinellid sponges apparently did not reveal the presence of any unusual steroid structures^{S46} and the authors concluded that the main sterols were derived predominantly from dietary uptake. Much less lipid screening of sponge biomass from the class Hexactinellida has been performed to date, however, in comparison with the more commonly found demosponges so further analyses of these sponges is recommended.

While the common finding of low levels of 27-norsterols in demosponges is intriguing, at this stage we can only say that on balance, while there may well be a sponge contribution to the 27-norcholestanes in SOSB sediments, we cannot rule out the possibility that these predominantly result from cleavage of the side chain of other steroid components of higher carbon number steroids (C₂₇-C₃₀) under unusual diagenetic and catagenetic conditions. Indeed, equally high amounts of side-chain cleaved steranes (20-*n*-alkylpregnanes,

including 27-norsteranes), relative to the C₂₇-C₃₀ analogues have been found in Devonian-Mississippian black shales from Williston Basin and their petroleum products^{S54}. No 24-isopropylcholestanes were reported for these Paleozoic rocks and oils in sterane MRM analyses so we must assume that these were absent. Further screening of other modern demosponge species is required to elucidate whether 27-norcholesterols are ever found as major sterol components in sponge cells.

10. Caution when interpreting 24-isopropylcholestane biomarker records

The 24-*n*-propylcholestanes are molecular markers for marine pelagophyte algae^{S3} and so provide a benchmark for inputs of sponge biomass, relative to these algae, to sediments through geological time. Detection of very low abundances of 24-isopropylcholestanes, particularly where the ratio of 24-isopropylcholestane/24-*n*-propylcholestane is less than 0.5 should be interpreted with caution, however. Noise in MRM chromatogram baselines that arises from interfering compounds such as bacteriohopanes and tricyclic triterpanes can be integrated together with the real C₃₀ desmethyl sterane signal, particularly when absolute abundances of 24-isopropylcholestanes are extremely low i.e. less than 20 ppm of total saturates^{S1}.

Non-zero signal of 24-isopropylcholestanes in saturated hydrocarbon fractions can contain contributions from (i) abiotic chemical transformation of a proportion of 24-*n*-propylidenecholesterols (the most common sterol precursor in marine pelagophyte algae which largely get transformed into 24-*n*-propylcholestanes) into 24-isopropylcholestanes

during diagenesis and catagenesis (but more likely the former) since this precursor sterol has a double bond in the sidechain adjacent to the required reaction site, particularly in shale lithologies due to acid clay-catalyzed rearrangements, (ii) small inputs of these relative to 24-*n*-propylcholestanes^{S3} from marine pelagophyte algae (see Section 2), and (iii) contributions from baseline noise peaks resulting from poor signal/noise in the MRM window for C₃₀ steranes, which is exacerbated at high thermal maturity (for late-oil window and overmature rocks) and which can overestimate the true 24-iso /24-*n*-propylcholestane ratio when this ratio is low.

Partial transformation of a small portion of 24-*n*-propylidenecholesterol into 24-isopropylcholestanes is likely from diagenetic reactions and may explain why 24-*n*-propylcholestane is always more abundant than 24-isopropylcholestane in the usual background signal in restricted and marine sedimentary organic matter of all ages outside the Neoproterozoic-Ordovician time window (an average 24-iso / 24-*n*-propylcholestane ratio of 0.2 to 0.3). Olefin intermediates have been shown to be important in the abiotic formation of isoalkanes from linear chain alkylated precursors in ancient sediments and petroleum^{S55}. Diagenetic secondary reactions also lead to the alteration of regular hopane and sterane biomarker structures . The Huqf rocks from South Oman show low amounts of rearranged hopanes (neohopanes) and steranes (diasteranes) relative to regular analogues for rocks of oil-window thermal maturity^{S41} so the high values of 24-iso/24-*n*-propylcholestane from Huqf strata are unlikely to be produced from anomalously high degree of secondary transformation reactions. Furthermore, we stress that high values of

24-iso / 24-*n*-propylcholestane ratio have only been found to date in a temporal pulse from late Neoproterozoic to Ordovician age strata and their generated petroleum products.

So, when 24-isopropylcholestane/24-*n*-propylcholestane is around 0.3 or less in solvent extract analyses then this parameter cannot be used with confidence to unambiguously discern fossil demosponge inputs to sediments. We cannot rule out the possibility of sponge contributions to older rocks which generate low 24-iso / 24-*n*-propylcholestane (<0.5) on analysis, but, conversely, it is much more difficult to dismiss the possibility that other inputs (i- iii) are responsible for these low ratios.

Ratios of ≥ 0.5 are really needed for strong evidence (and in late Cryogenian to Early Cambrian rocks then values >1.0 are often found) with the proviso that C₃₀ regular sterane signal should be significantly higher than baseline noise in MRM chromatograms from which the ratios were measured. Accordingly, our data set better constrains the temporal record of elevated 24-isopropylcholestane signal reported previously from Neoproterozoic rocks and oils and which extends into the Ordovician in other marine sedimentary basins^{S1}.

11. Absence of significant amounts of 24-isopropylcholestanes in pre-Sturtian

Proterozoic sedimentary rock extracts

The first report of elevated levels of 24-isopropylcholestanes in Ediacaran-Cambrian carbonate rock extracts^{S1} also included a number of 24-iso / 24-*n*-propylcholestane ratios calculated from biomarker analyses of six pre-Sturtian-aged Proterozoic carbonate sediments

and shales, including *ca.* 850-800 Myr Bitter Springs Formation carbonates from the Amadeus Basin (Australia) and *ca.* 800-700 Myr Visingsö Group (Sweden) shale. In all cases (except one), ratios of <0.25 are found indicating that the low abundances of 24-isopropylcholestanes are not sufficient in these samples to unambiguously record fossil demosponge inputs. For a shale from the *ca.* 1640 Myr Yalco Formation from the McArthur Group (Australia), then the calculated biomarker ratio of 0.36 was slightly higher than the average background value of 0.3^{S1} (but still below our recommended conservative cut-off point of 0.5 to signify sponge input). From recent experience in analyzing sediments and kerogens from the mid-Proterozoic McArthur Basin (such as *ca.* 1640 Myr Barney Creek Formation dolostones and siltstones from McArthur Group^{S56} as well as *ca.* 1400 Myr Roper Group shales) we found the C₂₇-C₂₉ regular steranes were up to two orders of magnitude less abundant than the co-occurring bacteriohopanes and often difficult to discern as discrete peaks. Since these triterpanes and tricyclic terpenoids show signal responses in the sterane mass transitions, these compounds if sufficiently abundant, could interfere. In light of this, the one reported value of 0.36 for a pre-Sturtian Yalco Fm. bitumen^{S1} is anomalous as it may have resulted from interfering triterpenoids. Regardless, multiple analyses of different rocks from the same stratigraphic unit are needed to confirm the possibility of sponge input from the absolute abundances of 24-isopropylcholestanes and consistently high values of 24-iso / 24-*n*-propylcholestane ratio.

No discernible significant quantities of 24-isopropylcholestanes were apparent either in C₃₀ sterane MRM chromatograms published for extracts from core sediments from the *ca.* 1100 Myr Nonesuch Formation of the US Midcontinent Rift System^{S56}. Additionally, we

examined the biomarker content in solvent extracts obtained from four (shallow and deepwater) pre-Sturtian Neoproterozoic marine sedimentary rocks from outcrop from the Tanner, Carbon Canyon, Awatubi and Walcott Members of the *ca.* 770-742 Myr Chuar Group^{S57} from Grand Canyon (all supplied by Susannah Porter, UCSB). There was sufficient biomarker signal to discern sufficient C₃₀ regular steranes above noise for three samples (all except Carbon Canyon sample) and for these the 24-iso / 24-*n*-propylcholestane ratios calculated were below 0.2.

To date, there has been no convincing molecular biomarker evidence obtained unambiguously indicating demosponge input to any pre-Sturtian Neoproterozoic sediment. This apparently holds for shallow water as well as deep water marine environments, inferred from analysis of dolostones from the Awatubi and Walcott Members of the Chuar Group deposited just prior to the Sturtian glaciations and from analyses of Bitter Springs Formation carbonates^{S1}.

We also analysed two deep water black shales from Wallara-1 well (depths of 1286 and 1296 m) from the interglacial late Cryogenian Aralka Formation in Australia (deposited between the Sturtian and Marinoan glacials) and detected only trace quantities of possible 24-isopropylcholestanes in MRM chromatograms. Again 24-iso / 24-*n* ratio was <0.2 in the sample with sufficient signal in m/z 414->217 MRM chromatograms to discern C₃₀ steranes well above baseline noise. So, this suggests that demosponges had not synchronously colonized all benthic marine environments globally in the Cryogenian after the Sturtian glaciation. Shallow seafloors on the shelf of the SOSB in the late Cryogenian

provided a suitable habitat for establishing and sustaining early benthic communities of demosponges.

12. Timing of demosponge radiation relative to Neoproterozoic glaciations

The late Neoproterozoic was a period associated with unusual climate^{S58-S60}, global carbon cycling dynamics^{S61} and a protracted oxidation of the atmosphere and oceans^{S62-S64}. Mounting evidence supports the occurrence of up to three low-latitude glaciations during the Neoproterozoic period (between 750-580 Myr). Whether the climatic shock of Neoproterozoic glaciations and their aftermath could have significantly affected global biogeochemical cycling and directly influenced the evolutionary history of eukaryotes, as suggested by Hoffman and Schrag^{S60}, remains a controversial aspect of Earth history.

This molecular biomarker record of late Cryogenian demosponges from South Oman together and early Ediacaran metazoan body microfossils reported extending to 5 metres above an ash bed dated at 632 ± 0.6 Myr from the lower Doushantuo Formation rocks in China^{S65} together suggest the first appearance of animals occurred in the Neoproterozoic between the Sturtian and Marinoan glaciations events. No convincing free or kerogen-bound sponge biomarker evidence has yet been reported from pre-Sturtian age sediments.

Comparative genomics has shown that certain key signaling and adhesion gene families critical for animal development had already evolved in choanoflagellates, which are the closest-living single celled relatives of animals^{S66}, and the genetic tool kit required for animal development was assembled in the Proterozoic^{S67}. Importantly, preliminary

analyses of sterols in the choanoflagellate, *Monosiga brevicolis* have shown 24-isopropylcholestane steroid skeletons do not appear to be biosynthesized by this species^{S68}, supporting our interpretation that abundant amounts of 24-isopropylcholesterane biomarkers are likely tracking the radiation of demosponges and not choanoflagellates or other unicellular eukaryotes (other than a possibly very low contribution from marine paelaogophytes, see Section 2). It is possible then that some environmental constraint had to be overcome in the Neoproterozoic before any organism could adapt to achieve complex, integrated multicellularity involving specialized cell types, as found in animals.

The shallow marine waters found in the Cryogenian may have allowed dissolved oxygen concentrations to be elevated for the first time above a critical threshold and would have likely been a major factor in sustaining the metabolic requirements of early metazoans. Sponges are able to live at relatively low oxygen conditions in benthic environments as illustrated by the preferred modern habitat of hexactinellids on the continental slope, from 200 to 2,000 m water depth, which appears to have been established by the middle Cambrian^{S69} and by the recent finding of all 3 Poriferan classes in the modern deep Southern Ocean, including abundant and diverse families of Demospongiae at 2500 m water depth^{S70}.

Neoproterozoic sponges and other early metazoans feeding on dissolved or particulate marine organic matter could have contributed to the oxygenation of their own benthic environments as their ecological niche progressively expanded from shallow water into

deeper water environments^{S51}. The evolution and ecological dominance of Neoproterozoic sponges has, therefore, been proposed as an important positive feedback mechanism at least partially responsible for the progressive removal of dissolved organic carbon aiding ventilation of the global ocean^{S51}. A large reduced carbon pool may have constituted a redox buffer in early Ediacaran oceans hindering deep water ventilation and thus inhibiting establishment of complex benthic animal communities^{S30,S61}. A protracted oxygenation of the Ediacaran biosphere is consistent with an early appearance of basal metazoans, as recorded by our sponge steroid record, which significantly predates the first records of the enigmatic Ediacaran macrofossils (~575 Myr) and the later proliferation of complex bilaterian animals associated with the Cambrian explosion (~530 Myr).

13. Co-occurrence of high C₂₉ steranes (stigmastanes) and demosponge markers in SOSB

Neoproterozoic marine sediments and oils which contain abundant sponge steranes^{S1} often (but not always) exhibit an unusually high dominance of regular C₂₉ steranes (stigmastanes) in the C₂₆-C₃₀ carbon number range. Examples, other than SOSB sediments and oils, are Ediacaran to Early Cambrian sediments and oils from Siberia, Pakistan, and India which also possess abundant 24-isopropylcholestanes^{S1}. High stigmastane content in rocks and oils of this age probably reflect high inputs of chlorophyte (green) microalgae^{S68} primary producers in these marine environments. While stigmastanes have been reported from pre-Sturtian Neoproterozoic sediments and oils, including sediments from the Chuar Group and from the *ca.* 1100 Myr Nonesuch Formation^{S56}, cholestanes are as abundant as

stigmastanes in these cases. The earliest occurrence of pronounced stigmastane dominance (>50% of total C₂₆-C₃₀ steranes) that has been found for marine sediments is from our Ghadir Manquil Fm. sediments in the late Cryogenian from the SOSB (Tables S1 and S2). So, it appears that microbial primary productivity was dominated by chlorophytes at least at some locations in shallow ocean shelves after the Sturtian glaciation.

Importantly, sterols containing the 24-isopropylcholestane skeleton, which we are proposing as a molecular proxy for demosponges when abundant, importantly have never been found in any chlorophyte cultures. So, this co-occurrence of both biomarkers in SOSB probably reflects local ocean chemistry and marine redox structure which favoured the proliferation of both green algae and demosponges. It has been established empirically that green algal clades have higher iron requirements than for red algal clades from trace element analyses^{S71}. We speculate then that this selective high productivity of marine chlorophytes may reflect elevated dissolved iron availability (above the Phanerozoic average) in extensive and interconnected regions of the post-Sturtian ocean. It has been argued that iron-rich waters could have accumulated during the Sturtian glaciation(s) as a result of suppressed ocean-atmosphere chemical interactions^{S72}. Iron-rich^{S73} (possibly micromolar levels), low sulfate conditions^{S31,S63} in the ocean also implies lack of persistent sulfide-rich waters, which are toxic to eukaryotes. Benthic sponges and other basal animals may have been confined to the shallowest, ventilated shelf environments for much of the late Cryogenian and Ediacaran and their dead remains were likely transported into sediment depocenters by lateral sediment transport. Interestingly, beneficial effects have noted after

addition of iron (micromolar levels of Fe^{3+} in these experiments) on the proliferation of dissociated cells (primmorphs)^{S74}, rates of spiculation^{S74}, and possibly stem cell growth^{S75} for the marine demosponge, *Suberites domuncula*. The SOSB sedimentary setting generally represents a shallow and nutrient-rich shelf depositional environment, with low levels of dissolved oxygen available in the benthic zone of the shallowest parts of the shelf which sustained demosponge metabolism.

14. Other possible demosponge markers in SOSB

There is potentially other biomarker evidence for sponges biomarkers found throughout all the Huqf strata in our dataset. A series of C_{19} to C_{30} mid-chain methylalkanes^{S41,S76} (often called X-peaks, since the exact origin is unclear) are particularly prominent in the Late Ediacaran to Early Cambrian Ara and Athel Group rocks as well as other rocks and oils of this age^{S77}, but are also found in lower amounts relative to *n*-alkanes in all the underlying Nafun and Abu Mahara Group sedimentary rocks. Some workers have argued that these were likely produced by symbiont bacteria in demosponges^{S77,S78} although other bacterial origins have been proposed^{S79}. No exact match of X peak alkanes with lipid hydrocarbon skeletons in extant organisms has yet been obtained though and further lipid screening studies are required to identify possible source organisms for these fossil alkanes. The most convincing evidence for ancient sponge contributions to Huqf Supergroup strata in South Oman presently comes from the consistently high 24-iso / 24-n-propylcholestanes ratios reported in our study.

Supplementary References

- S1. McCaffrey, M. A. *et al.* Paleoenvironmental implications of novel C₃₀ steranes in Precambrian to Cenozoic Age petroleum and bitumen. *Geochimica et Cosmochimica Acta* **58**, 529 (1994).
- S2. Bowring, S. A. *et al.* Geochronologic constraints on the chronostratigraphic framework of the Neoproterozoic Huqf Supergroup, Sultanate of Oman. *American Journal of Science* **307**, 1097-1145 (2007).
- S3. Moldowan, J. M. *et al.* Sedimentary 24-*n*-propylcholestanes, molecular fossils diagnostic of marine algae. *Science* **247**, 309-312 (1990).
- S4. Love, G.D., Snape, C.E., Carr, A.D. & Houghton, R.C. Release of covalently-bound biomarkers in high yields from kerogen via catalytic hydrolysis. *Organic Geochemistry* **23**, 981-986 (2005).
- S5. Murray, I. P., Love, G. D., Snape, C. E. & Bailey, N. J. L. Comparison of covalently-bound aliphatic biomarkers released via hydrolysis with their solvent-extractable counterparts for a suite of Kimmeridge clays. *Organic Geochemistry* **29**, 1487-1505 (1998).
- S6. Kokke, W.C.M.C., Schoolery, J.N., Fenical, W. & Djerassi, C. Biosynthetic studies of marine lipids. 4. Mechanism of side chain alkylation in (E)-24 propylidenecholesterol by a chrysophyte alga. *Journal of Organic Chemistry* **49**, 3742-3752 (1984)
- S7. Giner, J.-L., Li, X. & Boyer, G. Sterol composition of *Aureoumbra lagunensis*, the Texas brown tide alga. *Phytochemistry* **57**, 787-789 (2001).

- S8. Rohmer, M., Kokke, W.C.M.C., Fenical, W. & Djerassi, C. Isolation of two new C₃₀ sterols. (24E)-24-*n*-propylidenecholesterol and 24-*n*-propylcholesterol, from a cultured marine chrysophyte. *Steroids* **35**, 219-231 (1980)
- S9. Raederstorff, D. & Rohmer, M. Sterols of the unicellular algae *Nematochrysoopsis roscoffensis* and *Chrysotila lamellose*: Isolation of (24E)-24-*n*-propylidenecholesterol and 24-*n*-propylcholesterol. *Phytochemistry* **23**, 2835-2838.
- S10. Giner, J.-L. & Boyer, G. Sterols of the brown tide alga *Aureococcus anophagefferens*. *Phytochemistry* **48**, 475-477 (1998).
- S11. Volkman, J.K. A review of sterol markers for marine and terrigenous organic matter. *Organic Geochemistry* **9**, 83-99 (1986).
- S12. Volkman, J.K. Sterols in microorganisms. *Applied Microbiology & Biotechnology* **60**, 495-506 (2003).
- S13. Giner, J.-L. & Djerassi, C. Biosynthetic studies of marine lipids. 31. Evidence for a protonated cyclopropyl intermediate in the biosynthesis of 24-propylidenecholesterol. *Journal of the American Chemical Society* **113**, 1386-1393.
- S14. Amthor, J. E., Grotzinger, J. P., Schroder, S., Bowring, S. A., Ramezani, J., Martin, M. W. & Matter, A. Extinction of Cloudina and Namacalathus at the Precambrian-Cambrian boundary in Oman. *Geology* **31**, 431-434 (2003).
- S15. Gorin, G. E., Racz, L. G. & Walter, M. R. Late Precambrian-Cambrian Sediments of Huqf Group, Sultanate of Oman. *AAPG Bull.-Am. Assoc. Petr. Geol.* **66**, 2609-2627 (1982).
- S16. McCarron, G. The sedimentology and chemostratigraphy of the Nafun Group, Huqf Supergroup, Oman. *PhD Thesis (Oxford University)*, 175 (2000).

- S17. Schröder, S., Schreiber, B. C., Amthor, J. E. & Matter, A. Stratigraphy and environmental conditions of the terminal Neoproterozoic-Cambrian period in Oman: evidence from sulphur isotopes. *Journal of the Geological Society* **161**, 489-499 (2004).
- S18. Loosveld, R. J. H., Bell, A. & Terken, J. J. M. The tectonic evolution of interior Oman. *GeoArabia (Manama)* **1**, 28-51 (1996).
- S19. Brasier, M., McCarron, G., Tucker, R., Leather, J., Allen, P., and Shields, G. New U-Pb zircon dates for the Neoproterozoic Ghubrah glaciation and for the top of the Huqf Supergroup, Oman. *Geology* **28**, 175-178 (2000).
- S20. Allen, P. A., Grotzinger, J. P., Le Guerroue, E., Cozzi, A., al Siyabi, H. & Newall, M. Neoproterozoic Geology of the Jebel Akhdar and Core from *Subsurface Field Guide, IAS 2005*, Muscat, Oman (2005).
- S21. Le Guerroue, E., Allen, P. & Cozzi, A. Two distinct glacial successions in the Neoproterozoic of Oman. *GeoArabia* **10**, 17-34 (2005).
- S22. Allen, P. A., Leather, J. & Brasier, M. D. The Neoproterozoic Fiq glaciation and its aftermath, Huqf supergroup of Oman. *Basin Research* **16**, 507-534 (2004).
- S23. Leather, J., Allen, P. A., Brasier, M. D. & Cozzi, A. Neoproterozoic snowball earth under scrutiny: Evidence from the Fiq glaciation of Oman. *Geology* **30**, 891-894 (2002).
- S24. Grotzinger, J. P., Al-Siyabi, A. H., Al-Hashimi, R. A. & Cozzi, A. New model for tectonic evolution of Neoproterozoic-Cambrian Huqf Supergroup basins, Oman. *GeoArabia* **7**, 241 (2002).

- S25. Le Guerroue, E., Allen, P. A. & Cozzi, A. Chemostratigraphic and sedimentological framework of the largest negative carbon isotopic excursion in Earth history: The Neoproterozoic Shuram Formation (Nafun Group, Oman). *Precambrian Research* **146**, 68 - 92 (2006a).
- S26. Mattes, B. W. & Conway-Morris, S. Carbonate/evaporite deposition in the Late Precambrian–Early Cambrian Ara Formation of southern Oman. In: Robertson, A. H. F., Ed2, Ed3, Ed4, Ed5, and Ed6 Eds.), *The geology and tectonics of the Oman region*. Geological Society, London (1990).
- S27. Le Guerroue, E., Allen, P. A., Cozzi, A., Etienne, J. L. & Fanning, M. 50 million year duration negative carbon isotope excursion in the Ediacaran ocean. *Terra Nova* **18**, 147 - 153 (2006b).
- S28. Bowring, S. A., Myrow, P. M., Landing, E. & Ramezani, J. Geochronological constraints on terminal Neoproterozoic events and the rise of Metazoans. *Astrobiology* **2**, 457 (2002).
- S29. Burns, S. J. & Matter, A. Carbon isotopic record of the latest Proterozoic from Oman. *Eclogae Geologicae Helvetiae* **86**, 595-607 (1993).
- S30. Fike, D. A., Grotzinger, J. P., Pratt, L. M. & Summons, R. E. Oxidation of the Ediacaran Ocean. *Nature* **444**, 744 - 747 (2006).
- S31. Calver, C. R. Isotope stratigraphy of the Ediacarian (Neoproterozoic III) of the Adelaide Rift Complex, Australia, and the overprint of water column stratification. *Precambrian Research* **100**, 121-150 (2000).
- S32. Condon, D., Zhu, M., Bowring, S., Wang, W., Yang, A. & Jin, Y. U-Pb Ages from the Neoproterozoic Doushantuo Formation, China. *Science* **308**, 95 - 98 (2005).

- S33. Halverson, G. P., Hoffman, P. F., Schrag, D. P. & Kaufman, A. J. A major perturbation of the carbon cycle before the Ghaub glaciation (Neoproterozoic) in Namibia: Prelude to snowball Earth? *Geochemistry Geophysics Geosystems* **3** (2002).
- S34. Halverson, G. P., Hoffman, P. F., Schrag, D. P., Maloof, A. C. & Rice, A. H. N. Toward a Neoproterozoic composite carbon-isotope record. *Geological Society of America Bulletin* **117**, 1181-1207 (2005).
- S35. Kaufman, A. J., Corsetti, F. A. & Varni, M. A. The effect of rising atmospheric oxygen on carbon and sulfur isotope anomalies in the Neoproterozoic Johnnie Formation, Death Valley, USA. *Chemical Geology* **237**, 47 - 63 (2007).
- S36. Workman, R. K., Grotzinger, J. P. & Hart, S. R. Constraints on Neoproterozoic ocean chemistry from $\delta^{13}\text{C}$ and $\delta^{11}\text{B}$ analyses of carbonates from the Witvlei and Nama Groups, Namibia. *Geochim. Cosmochim. Acta* **66**, 847 (2002)
- S37. Grotzinger, J. P., Bowring, S. A., Saylor, B. Z. & Kaufman, A. J. Biostratigraphic and geochronological constraints on early animal evolution. *Science* **270**, 598-604 (1995).
- S38. Schröder, S., Schreiber, B. C., Amthor, J. E. & Matter, A. A depositional model for the terminal Neoproterozoic - Early Cambrian Ara Group evaporites in south Oman. *Sedimentology* **50**, 879-898 (2003).
- S39. Schröder, S. & Grotzinger, J. P. Evidence for anoxia at the Ediacaran-Cambrian boundary: the record of redox-sensitive trace elements and rare earth elements in Oman. *J. Geol. Soc.* **164**, 175-187 (2007).

- S40. Amthor, J. E., Ramseyer, K., Faulkner, T. & Lucas, P. Stratigraphy and sedimentology of a chert reservoir at the Precambrian-Cambrian Boundary: the Al Shomou Silicilyte, South Oman Salt Basin. *GeoArabia* **10**, 89 - 122 (2005).
- S41. Grosjean, E., Love, G. D., Stalvies, C., Fike, D. A. & Summons, R. E. New oil-source correlations in the South Oman Salt Basin. *Organic Geochemistry* In Press (2008).
- S42. Farrimond, P., Love, G. D., Bishop, A. N., Innes, H. E., Watson, D. F. & Snape, C.E. Evidence for the rapid incorporation of hopanoids into kerogen. *Geochimica et Cosmochimica Acta* **67**, 1383-1394 (2003).
- S43. Bligh, E.G. & Dyer, W.J. A rapid method of total lipid extraction and purification. *Canadian Journal of Biochemistry and Physiology* **37**, 911-917 (1959).
- S44. Love G.D., Bowden S.A., Summons R.E., Jahnke, L.L., Snape C.E., Campbell C.N. & Day J.G. An optimised catalytic hydrolysis method for the rapid screening of microbial cultures for lipid biomarkers. *Organic Geochemistry* **36**, 63-82 (2005).
- S45. Itoh, K. Minor and trace sterols in marine invertebrates. Part 35. Isolation and structure elucidation of seventy four sterols from the sponge *Axinella canniba*. *Journal of the Chemical Society Perkin Transactions I*, 147-152 (1983).
- S46. Bergquist, P.R., Hofheinz, W. & Oseterhelt, G. Sterol composition and the classification of the Demospongiae. *Biochemical Systematics and Ecology* **8**, 423-435 (1980).
- S47. Rampen, S.W., Schouten, S., Abbas, B., Elda Panato, F., Muyzer, G., Campbell, C.N., Fehling, J. & Sinninghe Damsté, J.S. On the origin of 24-norcholestanes and the use as age-diagnostic biomarkers. *Geology* **35**, 419-422 (2007).

- S48. RambaBu, M., Sarma, N.S. & Nittala, S. Chemistry of herbacin and new unusual sterols from the marine sponge *Dysidea herbacea*. *Indian J. Chem.* **26B**, 1156-1160 (1987).
- S49. Holfheinz, W. & Oesterhelt, G. 24-Isopropylcholesterol and 22-Dehydro-24-isopropylcholesterol, novel sterols from a sponge. *Helvetica Chimica Acta* **62**, 1307-1309 (1979).
- S50. Li, C.-W., Chen, J.-Y., & Hua, T.-E. Precambrian sponges with cellular structures. *Science* **279**, 879-882 (1998).
- S51. Sperling, E. A., Peterson, K. J. & Pisani, D. in *The Rise and Fall of the Ediacaran Biota* (eds. Vickers-Rich, P. & Komarower, P.) 355-368 (Geological Society Special Publications, London, 2007).
- S52. Lawson, M.P., Stoilov, I., Thompson, J.E. & Djerassi, C. Cell membrane location of sterols with conventional and unusual side chains in two marine demosponges. *Lipids* **23**, 750-754 (1988).
- S53. Blumenberg, M., Thiel, V., Pape, T., & Michaelis, W. The steroids of hexactinellid sponges. *Naturwissenschaften* **89**, 415-419.
- S54. Li, M. & Jiang, C. Bakken/Madison petroleum systems in the Canadian Williston Basin. Part 1: C₂₁-C₂₆ 20-*n*-alkylpregnanes and their triaromatic analogs as indicators for Upper Devonian-Mississippian epicontinental black shale derived oils? *Organic Geochemistry* **32**, 667-675 (2001).
- S55. Kissin, Y.V. Catagenesis and composition of petroleum: Origin of *n*-alkanes and isoalkanes in petroleum crudes. *Geochimica et Cosmochimica Acta* **51**, 2445-2457 (1986).

- S56. Brocks, J.J., Love, G.D., Summons, R.E., Knoll, A.H., Logan, G.A. & Bowden, S.A. Biomarker evidence for green and purple sulphur bacteria in a stratified Palaeoproterozoic sea. *Nature* **437**, 866 (2005).
- S56. Pratt, L.M., R.E. Summons & Hieshima, G.B. Sterane and triterpane biomarkers in the Precambrian Nonesuch Formation, North American Midcontinent Rift. *Geochimica et Cosmochimica Acta* **55**, 911-916.
- S57. Dehler, C.M. *et al.* High resolution $\delta^{13}\text{C}$ stratigraphy of the Chuar Group (ca. 770-742 Ma), Grand Canyon: Implications for mid-Neoproterozoic climate change. *GSA Bulletin* **117**, 32-35 (2005).
- S58. Hoffman P. F., Kaufman A. J. Halverson G. P. & Schrag D. P. (1998) A Neoproterozoic snowball earth. *Science* **281**, 1342-1346 (1998).
- S59. Evans, D. A. D. Stratigraphic, geochronological, and paleomagnetic constraints upon the Neoproterozoic climatic paradox. *American Journal of Science* **300**, 347-433 (2000).
- S60. Hoffman, P. & Schrag, D.P. The snowball Earth hypothesis: testing the limits of global change. *Terra Nova* **14**, 129-155 (2002).
- S61. Rothman D. H., Hayes J. M. & Summons R. E. Dynamics of the Neoproterozoic carbon cycle. *Proc. Natl Acad. Sci. USA* **100**, 8124-8129 (2003).
- S62. Des Marais, D. J., Strauss H., Summons, R. E. & Hayes, J. M. Carbon isotope evidence for the stepwise oxidation of the Proterozoic environment. *Nature* **359**(6396), 605-609 (1992).

- S63. Kah, L.C., Lyons, T. W. & Frank, T. D. Low marine sulphate and protracted oxygenation of the proterozoic biosphere. *Nature* **431**, 834-838 (2004).
- S64. Canfield, D.E., Poulton, S.W. & Narbonne, G.M. Late-Neoproterozoic deep-ocean oxygenation and the rise of animal life. *Science* **315**, 92-95 (2007).
- S65. Yin, L. et al. Doushantuo embryos preserved inside diapause egg cysts. *Nature* **446**, 661-633 (2007).
- S66. King, N. The unicellular ancestry of animal development *Developmental Cell* **7**, 313-325 (2004).
- S67. Knoll, A.H. & Carroll, S.B. Early animal evolution: Emerging views from comparative biology and geology. *Science* **284**, 2129-2137 (1999).
- S68. Kodner, R. B., Summons, R. E., Pearson, A., King, N. & Knoll, A. H. Sterols in a unicellular relative of the metazoans. *Proc. Natl Acad. Sci USA* **105**, 9897-9902.
- S69. Wu, W., Yang, A.-H., Janussen, D., Steiner, M., and Zhu, M.-Y. Hexactinellid sponges from the Early Cambrian black shale of South Anhui, China. *Journal of Paleontology* **79**, 1043-1051 (2005).
- S70. Janussen, D., and Secher Tendal, O. Diversity and distribution of Porifera in the bathyal and abyssal Weddell Sea and adjacent areas. *Deep Sea Research Part II: Topical Studies in Oceanography* **54**, 1864-1875 (2007).
- S71. Falkowski, P.G. et al. The evolution of modern eukaryotic phytoplankton. *Science* **305**, 354-360 (1994).
- S72. Kirschvink, J.L. Late Proterozoic low-latitude global glaciations: the snowball earth. in *The Proterozoic Biosphere* (eds.Schopf, J.W.& Klein, C..) 51-52 (Cambridge University Press, Cambridge, 1992).

- S73. Canfield, D.E. *et al.* Ferruginous conditions dominated later Neoproterozoic deep-water chemistry. *Science* **321**, 949-952 (2008)
- S74. Krasko, A. *et al.* Iron induces proliferation and morphogenesis in Primmorphs from the marine sponge, *Suberites domuncula*. *DNA and Cell Biology* **21**, 67-80.
- S75. Müller, W.E.G., Korzhev, M., Le Pennec, G., Müller, I.M. & Schröder, H.C. Origin of metazoan stem cells in sponges: first approach to establish the model (*Suberites domuncula*). *Biomolecular Engineering* **20**, 369-379 (2003).
- S76. Höld I.M., Schouten S., Jellema J. and Sinninghe Damsté, J.S.. Origin of free and bound mid-chain methyl alkanes in oils, bitumens and kerogens of the marine, Infracambrian Huqf Formation (Oman). *Organic Geochemistry* **30**, 1411-1428 (1999).
- S77. Peters, K.E., Walters, C.C. & Moldowan, J.M. In *The Biomarker Guide Volume 2* 771-772 (Cambridge University Press, UK, 2005).
- S78. Thiel, V. *et al.* Mid-chain branched alkanolic acids from "living fossil" demosponges: a link to ancient sedimentary lipids? *Organic Geochemistry* **30**, 1-14 (1999).
- S79. Love, G.D., Stalvies, C., Grosjean, E., Meredith, W. & Snape, C.E. Analysis of molecular biomarkers covalently bound within Neoproterozoic sedimentary kerogen. In *From Evolution to Geobiology: Research Questions Driving Paleontology at the Start of a New Century* (eds. Kelley, P.H. & Bambach, R.K.) 67-83 (Paleontological Society Short Course, October 4, 2008. Paleontological Society Papers, Vol. 14, 2008).

- S80. Borchiellini, C., Chombard, C., Manuel, M., Alivon, E., Vacelet, J. & Le Parco, Y. Molecular phylogeny of Demospongiae: implications for classification and scenarios for character evolution. *Molecular Phylogenetics and Evolution* **32**, 823-837 (2004).
- S81. Wünsche, L., Gülaçar, F. O. & Buchs, A. Several unexpected marine sterols in a freshwater sediment. *Organic Geochemistry* **11**, 215-219 (1987).
- S82. Dembitsky, V. M., Rezanka T. & Srebink M. Lipid compounds of freshwater sponges: family Spongillidae, class Demospongiae. *Chemistry and Physics of Lipids* **123**, 117-155 (2003).

Table S1: Selected biomarker ratios and yields obtained from free saturate fractions of sediment cores and cuttings

Well ID	Min. Depth (m)	Strat.	Ster/hopane ^a	%C26 ster ^b	%C29 ster ^c	%C30 ster ^d	i-C30/n-C30 ^e	27-nor/24-iso ^e	27-nor ^e ppm sats	24-iso ^e ppm sats
MKS-2	1648	A6C	0.82	6.46	58	2.05	1.15	4.01	556.0	138.7
SAR-2	3838	A6C*	0.21*	6.88*	69	6.69*	1.95	1.04	68.6	65.6
AJB-1	3588	A5C*	0.22*	9.96*	62	1.89*	0.95	5.03	65.2	13.0
OMR-1	2851	A5C	0.85	6.62	69	1.93	1.55	2.85	67.0	23.5
OMR-1	2853	A5C	0.82	4.81	69	2.02	1.67	2.48	43.9	17.7
BB-3	2920	A4C	0.97	4.84	68	2.45	1.44	4.22	21.2	5.0
BB-3	2928	A4C	0.91	4.86	70	2.11	1.49	3.23	23.3	7.2
BB-3	2930	A4C	1.05	6.26	68	2.45	1.36	4.08	47.3	11.6
BB-5	3009	A4C	0.99	4.36	66	1.95	1.39	5.37	49.4	9.2
BB-2	2927	A3C	0.96	4.73	75	2.10	1.49	3.17	44.3	13.5
BBN-1	3785	A3C	0.79	5.92	70	2.02	1.38	3.12	153.1	49.0
BBN-1	3787	A3C	0.87	12.7	69	2.31	1.46	2.80	33.1	11.8
BBN-1	3789	A3C	0.78	5.36	71	2.10	1.66	2.12	50.7	23.9
BBN-1	3790	A3C	0.82	3.92	70	2.10	1.67	1.98	50.6	25.5
DRR-1	2969	A3C	0.82	4.77	70	2.00	1.45	3.19	175.5	55.0
DRR-1	2990	A3C	0.78	4.56	70	2.07	1.60	2.87	179.5	62.5
BBN-1	4204	A2C	0.96	6.03	75	2.13	1.52	3.10	39.4	9.5
RF-1	3547	A2C*	0.57	12.9*	70	3.56*	1.17	2.41	96.4	39.9
RF-1	3577	A2C*	0.59	10.1*	72	4.65*	1.48	1.62	93.5	57.7
SAB 1	2399	A2C	0.93	4.46	75	1.90	1.69	2.78	33.2	11.9
SJT-1	5033	A2C	0.72	4.94	52	2.84	1.26	1.81	49.7	27.4
SJT-1	5053	A2C	0.83	4.74	61	3.39	1.77	1.45	49.3	33.9
DHS-3	2997	A1C	0.72	4.52	73	1.80	1.92	3.17	249.1	78.6
MIN-1	3400	A1C*	0.52*	9.88*	73	4.75*	1.42	1.85	109.8	59.4
MIN-1	3430	A1C*	0.54*	9.62*	71	5.20*	1.49	2.24	261.3	116.7
AMSE-1	2345	Buah	0.76	4.07	73	1.66	0.86	5.97	34.7	5.8
SB-1	1569	Buah	0.74	8.04	72	1.33	0.77	8.09	88.4	10.9
TRF-2	4411	Buah	0.84	7.39	67	1.74	0.70	8.23	71.5	8.7
ATH-1	2016	Buah	1.06	9.16	64	1.82	0.55	9.08	193.3	21.3
ZFR-1	1905	Shuram	0.61	6.27	71	2.33	1.78	2.74	253.5	92.6
ATH-1	2379	Shuram	0.56	3.02	77	2.01	0.81	2.57	280.0	109.1
ATH-1	2053	Shuram	0.96	3.81	68	2.12	0.92	5.42	75.9	14.0
ATH-1	2424.5	Shuram	0.66	2.86	70	2.19	1.10	2.75	18.7	6.8
ATH-1	2449	Shuram	0.70	6.68	65	2.50	1.41	2.76	22.2	8.0
TF-1	2247.5	Shuram	1.06	6.17	65	1.87	1.07	5.76	197.3	34.3
TM-6	2350	Shuram	1.00	5.63	70	2.18	0.92	3.25	115.8	35.6
TM-6	2685	Shuram	0.80	6.15	70	2.00	1.33	2.29	59.7	26.1
TM-6	2800	Khufai	0.84	5.17	73	2.02	1.27	4.19	182.2	43.5
TM-6	2830	Khufai	0.49	6.02	72	3.34	1.43	2.68	193.7	72.3
RNB-1	3125	Masirah B	0.49	6.84	58	3.53	3.98	1.54	22.3	14.5
ZFR-1	2280	Masirah B	0.73	5.18	84	12.61	16.1	0.43	104.7	245.7

SRS -1	4230	Masirah B	0.70	5.70	64	2.25	1.49	2.93	18.0	6.1
TM-6	2895	Masirah B	0.70	4.49	69	3.16	1.35	2.03	24.4	12.1
MWB-1	2628	Masirah B	0.73	4.86	60	2.44	1.52	3.86	63.7	16.5
GM-1	2420	Ghad. Manquail	0.90	7.18	72	2.65	3.26	3.11	189.4	61.0
MQR-1	4370	Ghad. Manquail	0.43	4.32#	56#	3.72#	0.52#	1.17#	n.d.	n.d.
Athel Group										
AML-9	1731	Thuleilat	0.95	11.4	60	2.78	1.34	7.25	575.3	79.3
ATH-1	1000	Thuleilat	0.62	5.74	67	3.34	1.36	4.42	80.6	18.3
MAR-248	2068	Thuleilat	1.29	5.41	71	1.91	1.37	7.49	260.5	34.8
TLT-2	1417.5	Thuleilat	0.81	4.86	71	2.23	1.35	5.38	134.3	24.9
TLT-2	1520	Thuleilat	0.91	5.16	73	2.27	1.56	4.48	158.6	35.4
ATH-1	1198	Silicylite	0.79	4.06	74	1.85	1.39	4.69	293.5	62.6
MAR-248	2104	Silicylite	1.50	4.78	72	1.93	1.42	7.08	202.0	28.6
MAR-248	2240	Silicylite	1.02	4.93	76	1.84	1.87	4.08	249.1	61.0
TLT-2	1551	Silicylite	1.21	6.11	74	2.41	2.13	3.69	331.9	90.0
TLT-2	1628	Silicylite	0.87	21.4	75	2.25	2.44	2.74	283.6	103.5
ATH-1	1425	U shale	0.85	7.73	66	2.37	1.11	6.05	104.0	17.2
ATH-1	1527	U shale	1.00	4.69	61	2.64	0.93	6.59	65.7	10.0
ATH-1	1773	U shale	0.91	19.7	61	2.63	0.78	9.06	39.1	4.3
MAR-248	2420	U shale	0.79	7.24	60	2.90	1.35	5.16	45.0	8.7
TLT-2	1751	U shale	0.89	9.87	65	2.20	1.41	5.79	161.3	27.9

a: ratio of (C₂₇-C₂₉ steranes)/(C₂₇+C₂₉₋₃₅ hopanes)

b: ratio of (21-nor- +27-norcholestanes)/Σ(C₂₆-C₂₉ steranes), for C₂₆ desmethylsteranes (C₂₇-C₂₉ 21-norsteranes peak areas were not included)

c: ratio of C₂₉ steranes to the total sum of C₂₇-C₂₉ steranes

d: : ratio of (24-*n*-propylcholestanes +24-isopropylcholestanes)/Σ(C₂₇-C₃₀ steranes) , for C₃₀ desmethylsteranes

e: ratios and compound yields were calculated from summing peak areas of all 4 regular isomers of each compound (αααS, αββR, αββS, aaaR)

#: affected by contamination from marine Phanerozoic-sourced petroleum drilling fluids, hence the lower ratios of %C₂₉ sterane and iso-C₃₀/n-C₃₀ sterane

*: saline marine facies, hence lower sterane/hopane ratio and apparently higher %C₂₆ and %C₃₀ steranes (as C₂₈ and C₂₉ 21-norsteranes, prominent at higher salinity, are not included in the calculation)

n.d. not determined

Analytical errors for absolute yields of 27-norcholestanes and 24-isopropylcholestanes absolute yields are estimated at ± 30%. Average uncertainties in hopane and sterane biomarker ratios are ± 8% as calculated from multiple analyses of a saturated hydrocarbon fraction prepared from an AGSO standard oil (n = 30 MRM analyses).

Table S2: Selected biomarker ratios and yields obtained from hydropyrolysis of kerogens/extracted sediments

Well ID	Min. Depth (m)	Strat.	Ster/hopane ^a	%C26 ster ^b	%C29 ster ^c	%C30 ster ^d	i-C30/n-C30 ^e	27-nor/24-iso ^e	27-nor ^e ppm sats	24-iso ^e ppm sats
OMR-1	2851	A5C	0.89	5.62	59	2.27	0.83	4.75	293.5	61.8
BB-3	2928	A4C	0.84	8.27	53	3.60	0.73	5.59	82.1	14.7
DRR-1	2990	A3C	0.80	7.99	62	1.88	0.82	8.89	138.3	15.6
RF-1	3547	A2C*	0.62	4.68	68	2.87	0.84	2.99	25.0	8.4
SJT-1	5033	A2C	0.93	9.80	52	3.16	0.64	6.83	35.6	5.2
SJT-1	5053	A2C	1.04	10.1	55	3.64	1.10	4.77	26.6	5.6
DHS-3	2997	A1C	0.77	6.42	69	2.88	0.96	4.10	76.2	18.6
MIN-1	3400	A1C*	0.58	3.98	70	2.15	1.35	2.62	30.3	11.6
SB-1	1569	Buah	0.89	12.9	63	1.34	0.53	29.2	129.8	4.4
AMSE-1	2345	Buah	1.12	10.5	67	1.91	0.72	14.1	59.2	4.2
ZFR-1	1905	Shuram	0.99	12.9	60	2.71	0.66	12.1	169.8	14.1
SNK-1	930	Shuram	0.55	13.3	58	4.58	1.35	5.20	14.1	2.7
JF-1	2648	Masirah B	0.73	14.2	55	5.60	1.35	4.03	15.1	3.8
HNR-1	2026	Masirah B	1.21	12.0	54	3.43	1.52	6.01	14.2	2.4
GM-1	2420	Ghad. Manquil	0.68	9.70	66	3.04	1.31	5.14	31.8	6.2
Athel Group										
AM-9	1731	Thuleilat	0.97	9.89	57	2.46	1.24	7.43	89.4	12.0
MAR-248	2068	Thuleilat	2.49	15.8	65	2.00	0.74	20.72	337.3	16.3
MAR-248	2104	Silicylite	2.10	12.4	69	2.25	0.69	14.65	163.3	11.2
MAR-248	2240	Silicylite	1.46	6.73	75	2.08	1.05	6.54	224.0	34.3
MAR-248	2420	U shale	1.19	13.2	53	2.71	1.66	8.35	79.4	9.5

a: ratio of (C₂₇-C₂₉ steranes)/(C₂₇+C₂₉₋₃₅ hopanes)

b: ratio of (21-nor- +27-norcholestanes)/Σ(C₂₆-C₂₉ steranes), for C₂₆ desmethylsteranes (C₂₇-C₂₉ 21-norsteranes peak areas were not included)

c: ratio of C₂₉ steranes to the total sum of C₂₇-C₂₉ steranes

d: ratio of (24-*n*-propylcholestanes +24-isopropylcholestanes)/Σ(C₂₇-C₃₀ steranes), for C₃₀ desmethylsteranes

e: ratios and compound yields were calculated from summing peak areas of all 4 regular isomers of each compound (αααS, αββR, αββS, aaaR)

n.d. not determined

*: saline marine facies

Analytical errors with 27-norcholestane and 24-isopropylcholestane absolute yields are estimated at ± 30%. Average uncertainties in hopane and sterane biomarker ratios are ± 8% as calculated from multiple analyses of a saturated hydrocarbon fraction prepared from an AGSO standard oil (n = 30 MRM analyses).

Note :- All products from HyPy were monitored to ensure that the bulk of the biomarkers generated were released by cleavage of covalent bonds and were not simply residual bitumen components. This was achieved by observing only very low or nil amounts of certain rearranged steranes and hopanes found exclusively as free hydrocarbons. For example, for all HyPy analyses here (Ts/Tm) <0.15, (diasteranes/regular steranes) <0.1 with much reduced levels of 28,30-bisnorhopanes relative to total hopanes compared with the corresponding free extracts.